Reviews of Electromagnetics, Vol. IV, 2025
EuCAP 2025 Special Issue
DOI: 10.53792/RoE/2025/25006

Reviews of Electromagnetics
EuCAP 2025 Special Issue

Low-Profile Lightweight X-Band PDHT Antenna for Earth Observation Satellite Constellations

Luca Di Palma[1]*, Davide Maiarelli[1]

Abstract
This paper presents the design, manufacturing and experimental characterization of a X-band Antenna (XBA) dedicated to Payload Data Transmission (PDT) for new Satellite platforms that will form constellations for Earth observation applications. The antenna is characterized by a reduced profile and minimized mass in order to fulfill stringent accommodation constraints, typical of Low Earth Orbit (LEO) medium-small platforms. Proposed design is based on a planar array of patch antennas implemented on a sandwich made of composite materials integrating also the antenna Beam Forming Network (BFN). Conducted and radiated measurements are carried out at different steps of an extensive space qualification campaign on first antenna model. The results demonstrate excellent RF performance fully in line with full-wave analysis. Furthermore, proposed technology is potentially attractive for a wide spectrum of LEO applications at different frequencies (e.g. GNSS, Inter-Satellite Links).

Key terms
Antenna Array; Microstrip Circuit; Patch Antenna; PDHT; Satellite Communications

[1] *Hardware Engineering Competence Center, Thales Alenia Space Italia, Rome, Italy*
***Corresponding author**: luca.dipalma@thalesaleniaspace.com

Received: 20/05/2025, Accepted: 10/08/2025, Published: 04/12/2025

1. Introduction

Earth observation Satellites play a fundamental role for many applications, such as Environmental monitoring, Weather forecast and Terrain mapping. In recent years, the development of LEO platforms for such applications enables the launch of a higher number of satellites forming large Constellations. Advantages from this approach are multiple. It is possible to introduce diversity in the embarked main instrument (SAR, Optic Payloads). A significant reduction of revisit time is possible, enabling an increased accuracy of measurements and, at the same time, enabling new applications [1]-[3].
In this frame, a new antenna working at X-band frequencies for Payload Data Handling and Transmission (PDHT) Sub-System is proposed. Its function is to allow the transmission of data collected by the satellite payload (e.g. radar images collected by embarked SAR antenna) to Earth stations. The antenna is a key element of this Satellite sub-system and its performance affect directly the transmission data rate [4]. The most adopted antenna architecture for such application is based on corrugated apertures fed by circular feeds [5]-[8]. They are characterized by an isoflux radiation pattern that provides higher gain at low elevation angles, compensating the increased path loss from atmospheric propagation. This kind of antenna is however characterized by a volume/weight that are not compatible with small LEO platforms and are destined to higher altitude satellites (MEO/GEO platforms).
Pencil-beam antennas are more compact but needs dedicated pointing mechanism to maintain link with Earth station. Where possible, this mechanism is entrusted directly to spacecraft attitude systems, including propulsion and control moment gyroscopes (CMG).
To implement a single medium gain pencil beam at these frequencies, a horn antenna would represent the simplest solution [9]-[11]. The RF chain shall include a spline and/or stepped profile horn, chokes, polarizers for circular polarization generation and, eventually, a filter. Such a solution is characterized by excellent RF performance and manufacturing repeatability. The overall envelope and mass, however, are often not compliant with stringent small-platforms accommodation constraints. Reflector-based solutions that can be designed with different geometries (e.g. offset, dual onset, ring focus, etc.) and offer

additional degrees for fine tuning and optimization suffer for similar issues [12].
Antenna architectures in planar technology assure a minimization of occupied volume, making them the most attractive solution on Satellite small platforms. Slot-based ([13]) and patch-based ([14]) array antennas are the most adopted solutions.
In this paper, we propose a planar array solution based on Printed Circuit Board (PCB) technology combined with layers made of composite materials that allows obtaining a lightweight low-profile design compatible with LEO satellites for Earth observation applications. The solution is based on an array of patch antennas and integrates a full corporate BFN. The design has been validated by a proper set of full-wave simulations and verified with a multi-step full space qualification campaign with realistic vibration and thermal loads. A prototype has been manufactured, assembled at tested at Thales Alenia Space facilities located in Rome and L'Aquila, Italy.
The paper is organized as follows. Section 2 provides a detailed description of the antenna architecture, starting from the key requirements considered as drivers for the preliminary trade-off to detailed analyses. Section 3 describes the phases needed for the manufacturing of the proposed Antenna. The experimental results obtained during the qualification campaign are reported in Section 4. Finally, some conclusions are drawn in Section 5.

2. Design Description

2.1. Requirements

In order to fulfill the satellite down-link communication at X-band frequency, the antenna needs to meet stringent requirements within an extended frequency band, taking into account thermal effects. The accommodation of the unit is critical and it has been selected taking into account EMC aspects at platform level [15]. The allocated volume is $22 \times 22 \times 3$ cm^3 with a mass of 500 gr. maximum. These are the most stringent requirements that have driven the antenna technology selection, as discussed in the previous section. It shall work in circular polarization (RHCP) between 8.05 and 8.35 GHz. This bandwidth has been already extended to take into account thermal effects. The XPD shall be higher than 25 dB. This requirement is not particularly demanding in general. However, considering the planar solution required, it should be carefully taken into account in the design process. In fact, polarization purity is a limit for such antennas and proper design strategy should be taken to assure the lowest cross polar levels. A Return Loss better than 18 dB is also requested.
The device should survive to harsh launch and operative space environments. In particular, a quite large temperature ranges between -65°C and +97°C is required with vibration levels of 27.6 G_{RMS} (maximum value on z axis, orthogonal to antenna plane). The design should be also ESD (Electrostatic Discharge) free. Proper selection of material and surface coatings should be put in place.
The antenna pointing to Earth Stations is handled at platform level during the downlink operative mode. Therefore, a pencil beam with minimum directivity of 24 dBi is specified within a Field of View (FoV) of 1°, excluding Beam Pointing Error (BPE). Budgets at Satellite Platform level provide additional 0.2° to be considered for BPE. Therefore, the FoV considered equal 1.4° (±0.7°) All the key requirements considered for the design are summarized in Table 1.

Table 1: XBA Antenna Requirements.

Parameter	Requirement
Envelope	$22 \times 22 \times 3$ cm^3
Mass	$<$ 500 gr.
Frequency Band	275 MHz at 8.2 GHz
Reflection Coefficient	$<$ -18 dB
Polarization	RHCP Single Pol.
XPD	$>$ 25 dB within FoV
Satellite Platform BPE	±0.2°
Field of View (FoV)	1.0° Full-Cone w/o BPE
Minimum Gain	$>$ 24 dBi within FoV
Max Gain variation	0.5 dB Peak-to-peak
Group Delay Variation	0.5 ns within Band
RF Interface	Coaxial SMA (Female)
Temperature Range	-65°C/+97°C
Random Vibration Levels	27.6 G_{RMS} Max

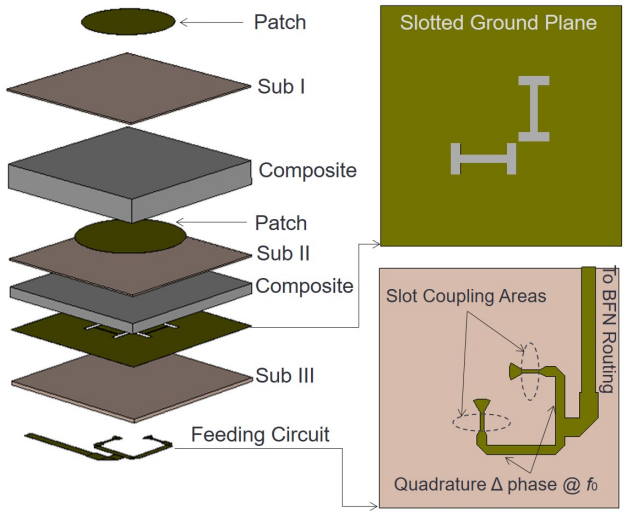

Figure 1: Sketch of the Radiating Element (RE) model developed for the XBA design: exploded view, feeding circuit layer and ground plane detailed views.

2.2. Radiating Element (RE) Design

The antenna can be divided in the following blocks, from the functional point of view:

- RE, based on patch technology.
- BFN circuitry, implemented in microstrip technology.

The proposed antenna configuration is based on an array of 64 Radiating Elements (RE) arranged in a regular 8×8 lattice in planar technology. The selected RE is composed by patch antennas in stacked configuration, as depicted in Fig. 1. The two patches, both with a circular shape, are excited by coupling through two "H"-shaped slots orthogonally placed on

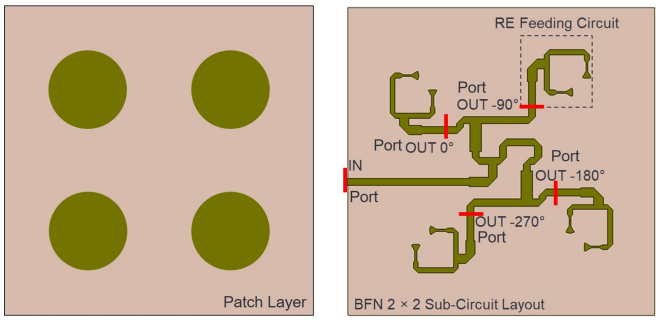

(a)

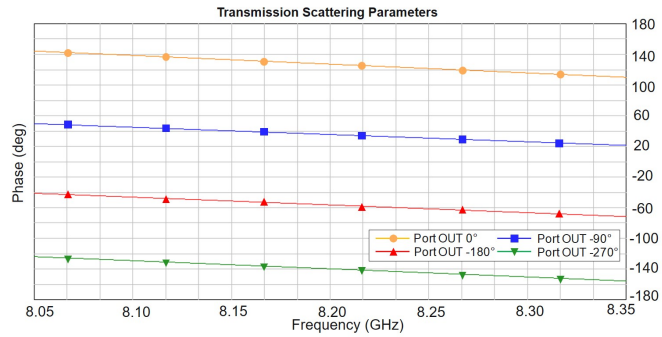

(b)

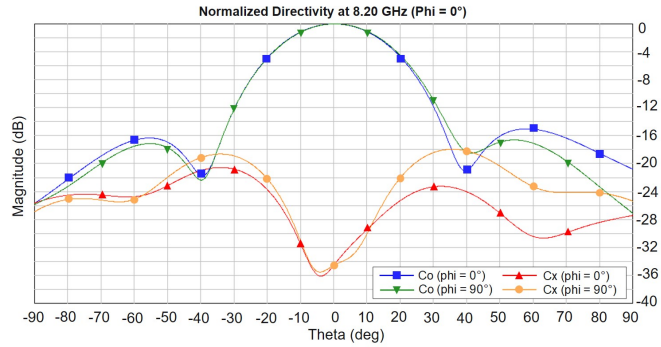

(c)

Figure 2: (2a) Sketch of the Quadruplet Antenna building block with back view showing BFN routing layout implemented in microstrip technology. (2b) Simulated Transmission Phases (S-parameters) calculated with full-wave FEM model. Refer to Fig. (2a) for port notation and location. (2c) Radiation patterns (Directivity) of Quadruplet sub-array obtained by exciting IN Port and removing the OUT ports (2a) calculated at the centre frequency (8.2 GHz) in the three principal planes

the ground plane. They are manufactured with high-precision PCB technology on two low-loss laminates sandwiched between a layer made of composite material. This stacking allows obtaining a minimization of RF losses and, at the same time, providing a significant reduction on mass. Furthermore, the resulting panel is characterized by high mechanical stiffness, which is compatible with harsh launch environmental conditions reflected in the high vibration loads.

Selected RE is compatible with double linear polarization and, by proper signal recombination, with circular polarization operation. Two open-ended stubs in microstrip lines are foreseen for slot feeding. Their width has been selected to maximize RF coupling with patches. This feeding circuitry is implemented on a third dedicated PCB on a low-loss high-frequency laminate substrate. All dielectric materials involved in the design are produced by Rogers Corp. [16]. A reactive splitter with balanced amplitudes and unbalanced phase outputs forms the feeding circuit ensuring quadrature-phase excitation of the two orthogonal linear polarizations (Fig. 1). Impedance output has been properly selected assuring sufficient room BFN routing of the whole array.

2.3. 2 × 2 Sub-Array Design

The described unit cell is integrated in a 2 × 2 sub-array, that will form the whole array building block (Fig. 2a). A rotation at step of 90° is applied between the four REs of the sub-array in order to apply sequential rotation technique [17]-[19]. Main benefit of this approach is the radiation performance improvement in terms of cross-polar discrimination. In fact, radiation pattern of single RE element described in the previous section is affected by the intrinsic asymmetry of the two orthogonally-placed slots. However, this choice allows to obtain a simple, compact and wide-band excitation of the fundamental modes of the patch. A proper feeding RF network has been therefore designed for equal-amplitude, quadrature phase excitation of the four RE. Circuit topology is based on a cascade of three reactive splitters, with impedance transformer sections and quadrature-phase differential line paths (Fig. 2a). Starting from the preliminary design of the single RE, the sub-array configuration has been optimized maintaining a full-wave approach. This choice allows to into account RF coupling between the RE elements and the microstrip BFN routing that implements the sequential rotation scheme.

The S-parameter transmission phases of the standalone circuit are shown in Fig. 2b. Obtained radiated performance demonstrate that cross polar component has been efficiently minimized (Fig. 2c). The obtained peak directivity spans from 14.0 to 14.7 dBi between 8.05 and 8.35 GHz, corresponding to an aperture efficiency larger than 90%. The cross polar discrimination (XPD) within FoV at boresight is better than 30 dB and Side Lobe Level (SLL) is better than -15.0 dB.

2.4. 8 × 8 Array Design

The optimized 2 × 2 sub-array described in the previous section has been arranged in an 8 × 8 regular lattice (Fig. 3a) with a spacing of 55 mm, corresponding to a RE inter-element spacing of 0.75 λ_0 at 8.2 GHz (27.5 mm). This spacing has been selected to fit the antenna allocated volume and the other key antenna requirements at sub-system level. The BFN needed to complete the design has been developed and implemented in microstrip technology on the same substrate that accommodate the RE excitations (Fig. 3a).

Additional steps of sequential rotations have been applied to further improve the radiation performance and reducing cross-polar levels. The result is the complete corporate distribution network shown in Fig. 3a. Starting from the input 50-Ohm microstrip line that can be interfaced with a standard coaxial connector [20], the developed layout is formed by a first bal-

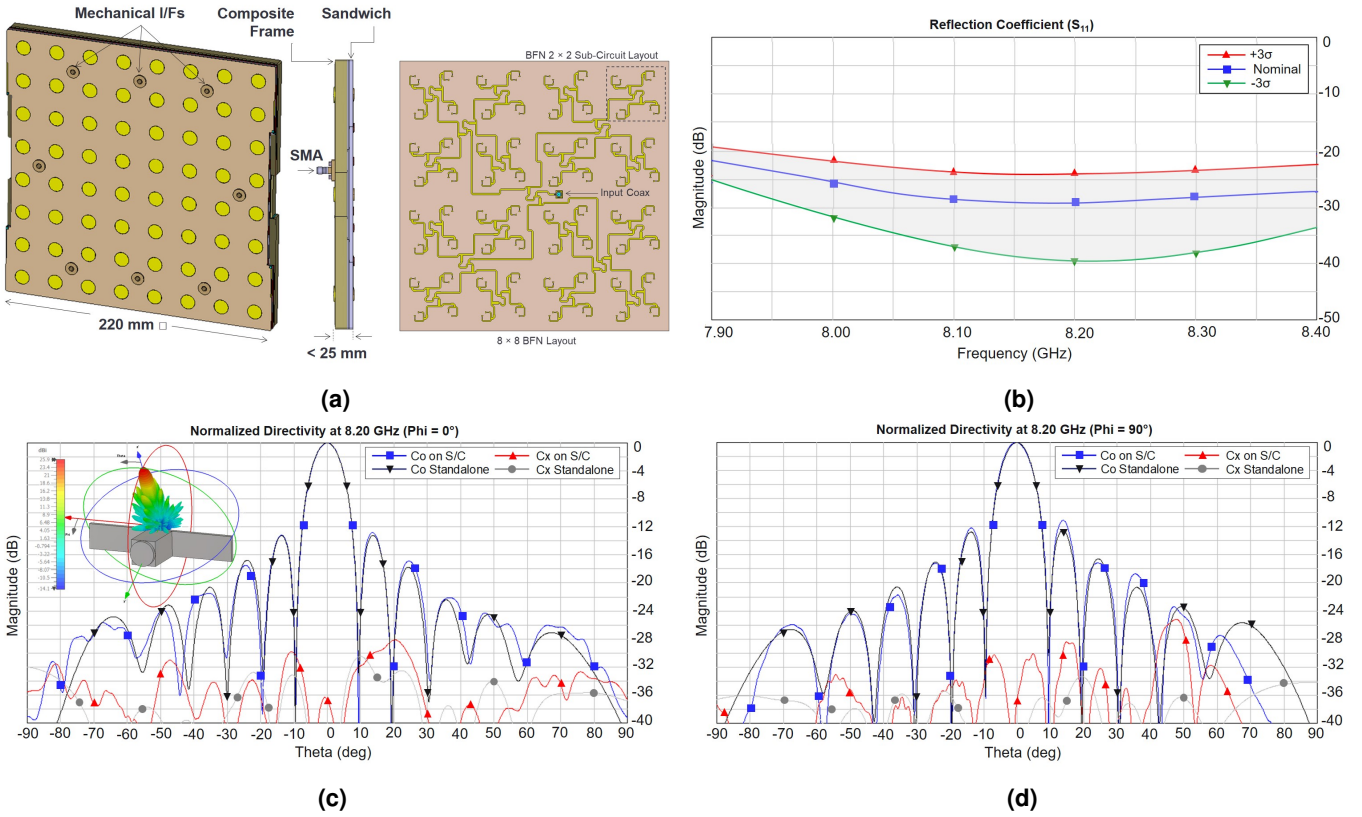

Figure 3: Sketch of the proposed X-band PDHT Antenna: (3a) front, side and with a back view showing BFN routing layout implemented in microstrip technology. (3b) Reflection coefficient at the antenna input (without coaxial connector) for nominal design and considering a Monte Carlo analysis on key manufacturing aspects: alignments of layer, etching precision and results are reported with for a confidence level of 3σ. Critical microstrip etched edges and alignment between the different layers have been considered in the sensitivity analysis. (3c, 3d) Calculated Radiation Pattern (Directivity) at 8.05 GHz with and without Scattering contribution from Spacecraft (3D model is reported in the inset of Fig. 3c).

anced four-way splitter with equal power division ratio and quadrature phase outputs. The four output lines have been connected to four division stages equal to the first one to reach each of the RE quadruplets forming the 64-element antenna layout. Similarly as already done for RE and 2×2 sub-arrays, all the circuit elements are taken into account in the modeling phase. Therefore, mutual coupling between closely spaced lines of the BFN, cross-coupling between lines and slots feeding the REs sections and coupling among circular patches of neighbor REs have been accurately taken into account in the calculations. Obtained reflection coefficient at the input microstrip line of the entire BFN circuit is better than 19.9 dB on the extended frequency band (Fig. 3b). SMA connector is not included in the full-wave calculations to save computational cost. On the other hand, matching of the connector is better than 30 dB at the XBA frequency range and its impact can be considered negligible. A dedicated sensitivity analyses are performed to assess the validity of the proposed solution considering involved manufacturing technologies. In particular, two key aspects are considered: the precision of the sizes of the critical elements from RF point of view and the misalignment between the different antenna layers. While the first aspect depends only by PCB etching precision, the second one depends on both PCB etching and implemented bonding process. The analyses are carried out considering full-wave simulation results applying a Monte Carlo Analysis with a standard deviation of 300 µm (layer misalignment) and 20 µm (PCB etching precision). Numerical results demonstrate that proposed solution is quite robust, assuring an Input Return Loss better than -19.0 dB (worst in-band value, 3-σ confidence level), as shown in (Fig. 3b).

A detailed full-wave model has been developed to predict the complete antenna performance. It includes all the antenna features, including mechanical frame, fixing screws and bushing. A proper set of full-wave simulations has been performed by means of state-of-the-art commercial EM software [21].

Radiation patterns are reported in Figs. 3c ,3d at the centre frequency (8.2 GHz) in the two principal planes ($\phi = 0°, 90°$). The achieved peak directivity equals 26 dBi, corresponding to an aperture efficiency of about 90%, with Half Power Beamwidth (HPBW) of 8.4°. Side lobes are below -12.5 dB. Within FoV (1.4°), the directivity drops by a factor of 0.2 dB. The XPD is better than 30 dB within the same angular range. Estimated losses are lower than 1 dB. No significant variation is obtained at the extreme frequencies within the band.

Further full-wave analyses are carried out to assess the impact of a Spacecraft on the radiation pattern. Due to large electrical sizes of the whole structure, the FEM model of the XBA has been combined with an integral equation solver optimizing the

computational costs. As shown in Figs. 3c, 3d, only a slight variation of SLL can be observed. No significant changes affect the pattern especially within targeted FoV at boresight.

2.5. Mechanical and Thermal Design Aspects

The proposed antenna RF design has been developed taking into account several mechanical constraints that are derived from unit requirements. In particular, a detailed FEM model has been developed to design and optimize the antenna supporting frame and its mechanical interfaces. The main challenge has been assuring that the antenna will survive to harsh conditions typical of satellite platform launching sequence respecting all other constraints (e.g. mass) and preserving the performance from functional point of view.

This fine optimization process leads to a robust and lightweight design with a first Eigen frequency of about 400 Hz fulfilling the vibration loads reported in the requirements. First main vibration mode-shapes calculated for the antenna installed on the supporting frame are shown in Fig. 4.

From thermal point of view, the Antenna has been analyzed considering a detailed model of the antenna taking into account all the thermo-physical properties of the involved materials. A realistic LEO orbit scenario at 7000 km. Proper protection will be provided with sunshield layer installed on the radiating aperture and by MLI blankets on the sides and rear parts of the Antenna Unit. The resulting temperature range seen at antenna level spans from -65°C to +97°C. All the materials and processes involved in the manufacturing are qualified to work in this temperature range.

3. EQM Manufacturing Process

An Engineering Qualification Model (EQM) has been manufactured (Fig. 5a) following the process described in this section. Patch layers and the BFN circuitry are RF-sensitive sub-parts, especially from dimensional point-of-view. They are all manufactured with high-precision etching process of PCB technologies on high-frequency laminates [16]. Selected material,

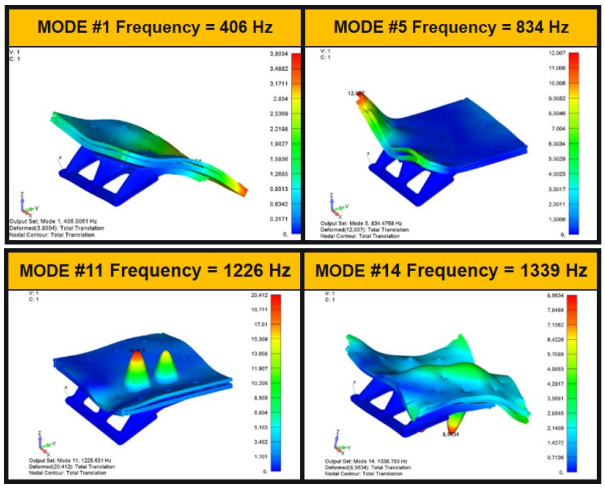

Figure 4: First vibration mode shapes and corresponding Eigen frequencies of the XBA Antenna unit installed on its supporting frame.

(a)

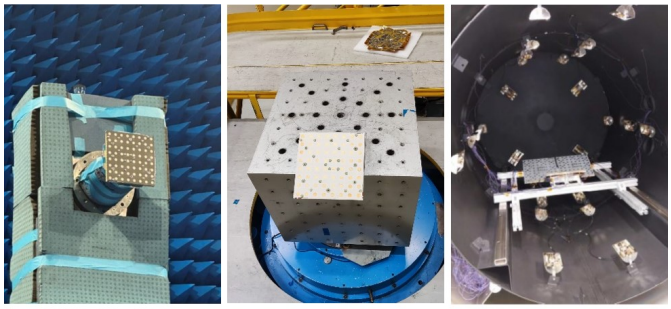

(b)

Figure 5: (5a) Photograph of Manufactured XBA EQM model. (5b) Photograph of XBA Antenna during qualification test campaign: Radiation Pattern setup in Anechoic Chamber, XBA mounted on shaker for Vibration Test and placed in Thermal Vacuum Chamber for cycling

processes and supplier are all space qualified. Manufacturing sequence and PCB finishing are chosen to meet the stringent RF requirements, especially in terms of Ohmic losses.

The obtained PCB are then assembled with composite layers by proper bonding process at controlled pressure and temperature with an in-house space qualified process.

Resulting PCB/composite sandwich is fixed on an ad-hoc frame by means of proper internal interfaces (bushings and pins). This frame, where external mechanical interfaces are foreseen (see Fig. 2), is manufactured with glass fiber by means of high-precision CNC machining. Finally, input coaxial connector is soldered on the antenna (Fig. 2).

The resulting panel is characterized by a very low density (about 5 Kg/m^2), allowing to meet the requirement on mass and assuring, at the same time, required stiffness.

4. Experimental Results and Qualification Campaign

The manufactured EQM model (Fig. 5a) has been fully verified with a space qualification campaign following the test matrix reported in Table 2. The Antenna has been mounted in the Near Field Test Rang (NFTR) for RF Tests, on a shaker for Vibration Test and in a Thermal Vacuum Chamber for cycling (Fig. 5b).

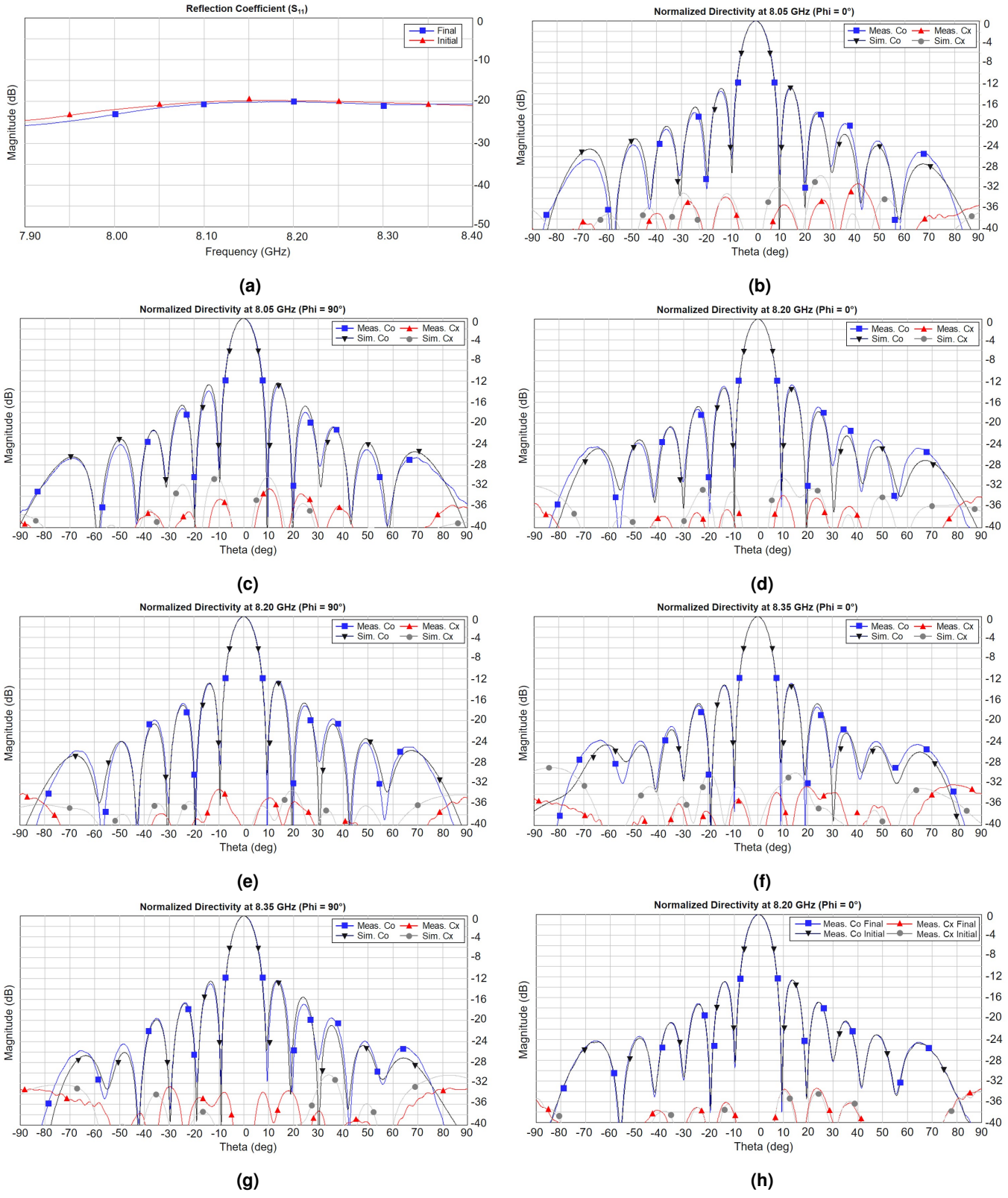

Figure 6: (6a) Measured S parameters (Input Return Loss) fo the XBA Antenna at the initial and final stages of the Qualification Campaign (see Table 2). Measurement data includes SMA connector. Simulated and Measured Radiation Patterns (Normalized Directivity) at (6b, 6c) 8.05 GHz, (6d, 6e) 8.20 GHz and (6f, 6g) 8.35 GHz in the horizontal (6b, 6d, 6f) and vertical planes (6c, 6e, 6g). (6h) Measured Radiation Patterns (Normalized Directivity) at 8.20 GHz in the horizontal plane at initial and final step phases of the test campaign (see Table 2).

Table 2: XBA Antenna Test Matrix.

Test	EQM	FM
Visual Inspection	●	●
Mass, Dimensional Check	●	●
Grounding Check	●	●
Return Loss (Initial)	●	●
Patterns and Gain (Initial)	●	●
Resonance Search	3 axes	1 axis[a]
Random vibration	3 axes	1 axis[a]
Visual Inspection	●	●
Return Loss (Intermediate)	●	●
Thermal Vacuum (four cycles)	●	●[a]
Return Loss (Final)	●	●
Patterns and Gain (Final)	●	●

[a] Test carried out considering Acceptance Levels.

After preliminary dimensional and mass checks, the antenna has been tested from RF point-of-view to verify initial conducted and radiated performance. At this stage, Reflection coefficient measurement demonstrate an excellent behavior with a maximum in-band value of -20 dB (Fig. 6a). Directivity patterns in circular polarization measured at center and side frequencies within the band are shown in Fig. 6b-6g. An excellent agreement between simulated and measured data can be observed on both co- and cross-polar components at all the frequencies. Excellent results are then obtained in terms of cross polar discrimination.

After successful completion of this phase, random vibrations test on three axes has been performed with in-plane/out-of-plane levels of 27.6 and 25.7 G_{RMS}, respectively. Thermal vacuum test (four cycles) has been performed between -65 °C and +97 °C. A comparison of measured Reflection Coefficients and Radiation Patterns before and after these environmental tests are reported in Figs. 6a, 6h. The curves are almost overlapped for all the frequencies and across the entire angular range. Finally, a complete inspection has been performed and no physical damages have been found. This excellent results validate the proposed design and confirms its mechanical stiffness.

A summary of the measured RF performance are summarized in Table 3. A minimum Directivity of 25.8 dBi has been verified experimentally at boresight. Gain measurements performed in Anechoic Chamber with substitution method confirms the full-wave predictions. It spans between 24.6 dBi and 24.8 dBi within the extended frequency band (8.05 – 8.35 GHz). The HPBW is 8.3° with a variation of 0.2° maximum. The cross polar discrimination is excellent (below -30 dB) within FoV, corresponding to an Axial Ratio better than 0.5 dB. Side Lobe Level are under -12.5 dB at all the frequencies in both principal planes. Finally, losses equal 1 dB maximum, confirming numerical predictions and design budget at sub-system level.

Table 3: XBA Antenna RF Performance Summary.

Parameter	Achieved Value	Remarks
Bandwidth	300 MHz	extended
Refl. Coeff.	$<$ -19.9 dB	Including SMA
Min. Dir.	$>$ 25.8 dB	Within FoV
HPBW	8.3° $+/-$ 0.2°	Across band
XPD	$>$ 30 dB	Within FoV
SLL	$<$ -12.5 dB	Both planes
Losses	1 dB	Ohmic, Mismatch

5. Conclusions

A low profile lightweight X-band Antenna for PDHT subsystems of LEO satellites for Earth Observation constellations has been introduced. It consists of an array of stacked patch antennas arranged in an 8 × 8 lattice, manufactured on a composite sandwich of PCBs. A full corporate feeding network based on sequential rotations has been developed in low-loss microstrip technology. The antenna meets the stringent requirements derived by the Subsystem for the envisaged satellite application, with focus on volume and mass savings, maintaining at the same time excellent RF performance within an extended thermal frequency band.

A full space qualification campaign representative of launch and orbit operations harsh environment has been successfully completed confirming predicted RF performance and validating the design. Proposed architecture can be also easily scaled to fit 1-U, 6-U 12-U CubeSat platforms for X-band communication and it can be easily adjusted in frequency to cover more small-platform satellite needs (e.g. Inter Satellite Links).

Acknowledgment

The Authors would like to thank all the colleagues from Thales Alenia Space involved in this project and, in particular: Mario Lanuti with his Team for the mechanical design of the antenna, Luca Giancaterini with his Team for the support provided in the definition of all the technological aspects and Daniele Cervelli with his Team for the performed measurement test campaign.

References

[1] G. Costa et al., ”IRIDE: The New Italian Space Programme”, *IGARSS 2024 - 2024 IEEE International Geoscience and Remote Sensing Symposium*, Athens, Greece, 2024, pp. 6663-6665.

[2] E. G. Cadau et al., ”The IRIDE Project: Satellites, Algorithms and Products of the New Italian Space Programme”, *IGARSS 2024 - 2024 IEEE International Geoscience and Remote Sensing Symposium*, Athens, Greece, 2024, pp. 6763-6766.

[3] F. Cotugno et al., ”An Innovative Orbital Configuration for Small Satellite SAR Constellations and Interferometric Applications: The Iride Case Study”, *IGARSS 2024 - 2024 IEEE International Geoscience and Remote Sensing Symposium*, Athens, Greece, 2024, pp. 6613-6617.

[4] B. Correia, S. Cunha, M. Zhou, V. Cristina, B. Byrne and P. M. Iglesias, ”Enhancing Data Downlink Performance with Beam Steerable Reflectarray Antennas”, *IGARSS 2023 - 2023 IEEE International Geoscience and Remote Sensing Symposium*, Pasadena, CA, USA, 2023, pp. 4494-4497.

[5] J. Wettergren, P. Dimming, J. F. Johansson and M. Öhgren, "A high gain X-band isoflux helix antenna," *10th European Conference on Antennas and Propagation (EuCAP)*, Davos, Switzerland, 2016.

[6] M. Kilian, C. Hartwanger, A. Schinagl-Weiß and M. Schneider, "X-band downlink antenna characterised by isoflux gain mask," *11th German Microwave Conference (GeMiC)*, Freiburg, Germany, 2018, pp. 21-24.

[7] F. Caminita et al., "A New Double Polarization Isoflux Antenna," *13th European Conference on Antennas and Propagation (EuCAP)*, Krakow, Poland, 2019.

[8] F. Caminita, E. Martini, G. Minatti, M. Sabbadini and S. Maci, "Low-Profile Dual-Polarized Isoflux Antennas for Space Applications," *IEEE Transactions on Antennas and Propagation*, vol. 69, no. 6, pp. 3204-3213, June 2021.

[9] K. Tomoki and H. Saito, "Dual circularly polarization antenna with High XPD for downlink communication of earth observation sateliite," *2017 IEEE Conference on Antenna Measurements and Applications (CAMA)*, Tsukuba, Japan, 2017, pp. 232-234.

[10] J. Galván and D. Colantonio, "Low back radiation compact antenna for data downlink in LEO satellites," *2009 SBMO/IEEE MTT-S International Microwave and Optoelectronics Conference (IMOC)*, Belem, Brazil, 2009, pp. 816-820.

[11] E. Kiraz, V. Akan, S. Çetinkaya, A. R. İçtihadi and B. Çolak, "X-Band Antenna with Electro-mechanical Steering Mechanism for IMECE Satellite," *2023 10th International Conference on Recent Advances in Air and Space Technologies (RAST)*, Istanbul, Turkiye, 2023.

[12] R. Mizzoni and F. Perrini, "Feasibility study on electronically steerable PDHT antenna S/S," *Proc. of the 5th Europ. Conf. on Ant. and Propag. (EUCAP)*, Rome, Italy, 2011, pp. 1157-1161.

[13] J. M. Fernandez Gonzalez, P. Padilla, G. Exposito-Dominguez and M. Sierra-Castaner, "Lightweight Portable Planar Slot Array Antenna for Satellite Communications in X-Band," *IEEE Antennas and Wireless Propagation Letters*, vol. 10, pp. 1409-1412, 2011.

[14] R. M. Hashmi and K. P. Esselle, "Planar high-gain antennas for direct broadcast satellite reception," *2016 IEEE 2nd Australian Microwave Symposium (AMS)*, Adelaide, SA, Australia, 2016, pp. 17-18.

[15] G. Galgani et al., "A Model for RF Coupling on Spacecraft Antennas," *2019 ESA Workshop on Aerospace EMC (Aerospace EMC)*, Budapest, Hungary, 2019.

[16] Rogers Corporation [Online] available: *www.rogerscorp.com*.

[17] P. S. Hall, "Application of sequential feeding to wide bandwidth circularly polarised microstrip patch arrays", *IEEE Proc. H Microw. Antennas Propag.*, vol. 136, no. 5, pp. 390-398, Oct. 1989.

[18] P. S. Hall and M. S. Smith, "Sequentially rotated arrays with reduced sidelobe levels", *IEEE Proc. Microw. Antennas Propag.*, vol. 141, no. 4, pp. 321-325, Aug. 1994.

[19] L. Di Palma, A. Clemente, L. Dussopt, R. Sauleau, P. Potier and P. Pouliguen, "Circularly Polarized Transmitarray With Sequential Rotation in Ka-Band," *IEEE Transactions on Antennas and Propagation*, vol. 63, no. 11, pp. 5118-5124, Nov. 2015.

[20] Rosenberger [Online] available: *www.rosenberger.com*.

[21] SIMULIA CST Studio Suite [Online] available: *www.3ds.com*.